Rapid report

New Phytologist

Rapid report

Shoot surface water uptake enables leaf hydraulic recovery in *Avicennia marina*

Tomás I. Fuenzalida[1], Callum J. Bryant[1], Leuwin I. Ovington[1], Hwan-Jin Yoon[2], Rafael S. Oliveira[3], Lawren Sack[4] and Marilyn C. Ball[1]

[1]Plant Science Division, Research School of Biology, The Australian National University, Acton, ACT 2601, Australia; [2]Statistical Consulting Unit, The Australian National University, Acton, ACT 2601, Australia; [3]Department of Plant Biology, Institute of Biology, University of Campinas – UNICAMP, Campinas, São Paulo CP 6109, Brazil; [4]Department of Ecology and Evolution, University of California Los Angeles, Los Angeles, CA 90095, USA

Author for correspondence:
Tomás I. Fuenzalida
Tel: +61 435390065
Email: tomas.fuenzalida@anu.edu.au

Received: *16 May 2019*
Accepted: *11 August 2019*

New Phytologist (2019) **224:** 1504–1511
doi: 10.1111/nph.16126

Key words: capacitance, drought, foliar water uptake, leaf hydraulic conductance, pressure–volume curve, recovery, shoot water uptake.

Summary

- The significance of shoot surface water uptake (SSWU) has been debated, and it would depend on the range of conditions under which it occurs. We hypothesized that the decline of leaf hydraulic conductance (K_{leaf}) in response to dehydration may be recovered through SSWU, and that the hydraulic conductance to SSWU (K_{surf}) declines with dehydration.
- We quantified effects of leaf dehydration on K_{surf} and effects of SSWU on recovery of K_{leaf} in dehydrated leaves of *Avicennia marina*.
- SSWU led to overnight recovery of K_{leaf}, with recovery retracing the same path as loss of K_{leaf} in response to dehydration. SSWU declined with dehydration. By contrast, K_{surf} declined with rehydration time but not with dehydration.
- Our results showed a role of SSWU in the recovery of leaf hydraulic conductance and revealed that SSWU is sensitive to leaf hydration status. The prevalence of SSWU in vegetation suggests an important role for atmospheric water sources in maintenance of leaf hydraulic function, with implications for plant responses to changing environments.

Introduction

There is a pressing need to understand the dynamics of loss and recovery of leaf hydraulic function in plants. Leaves represent a major (> 30%) fraction of the resistance to liquid water movement through entire plants (Sack & Holbrook, 2006). The efficiency of water transport through leaves, leaf hydraulic conductance (K_{leaf}), has indirect effects constraining gas exchange through its effects on stomatal conductance (Sack & Holbrook, 2006; Blackman *et al.*, 2009; Xiong *et al.*, 2017; Flexas *et al.*, 2018; Wang *et al.*, 2018), and is a critical determinant of plant productivity (Scoffoni *et al.*, 2016). Yet, K_{leaf} is strongly affected by plant hydration. As plants dehydrate, K_{leaf} declines due to changes in conductance within and outside the xylem tissue (Scoffoni *et al.*, 2017b), with the latter occurring at mild levels of water stress in association with decline in turgor. Because decline of K_{leaf} occurs at mild water stress, many plants experience diel cycles of loss and recovery of K_{leaf} (Bucci *et al.*, 2003; Lo Gullo *et al.*, 2003; Brodribb & Holbrook, 2004; Hao *et al.*, 2008; Johnson *et al.*, 2009; Yang *et al.*, 2012), and that recovery depends on the extent of dehydration (Blackman *et al.*, 2009; Brodribb & Cochard, 2009).

Many plants live in arid or saline environments in which low soil water potential may limit the extent of overnight K_{leaf} recovery, or where rehydration may be delayed by loss of conductance itself (i.e. a negative feedback response). In these cases, alternative water sources might enable rehydration leading to K_{leaf} recovery. Absorption of liquid water from the surface of aboveground organs, herein referred to as shoot surface water uptake (SSWU), is a water acquisition mechanism found in nearly all plant families (Dawson & Goldsmith, 2018). Despite its common occurrence, there are important knowledge gaps regarding the mechanisms and physiological consequences of SSWU (Berry *et al.*, 2018), and how these influence tree fitness. For example, recent evidence indicates that anisohydric species that rely strongly on SSWU are more vulnerable to drought and climate change than isohydric species with lower SSWU capacity (Eller *et al.*, 2016), suggesting a role for SSWU in maintenance of hydraulic function. While stem embolism refilling through SSWU has been observed in two conifer species (Mayr *et al.*, 2014; Mason Earles *et al.*, 2016), there are no experimental data on whether SSWU affects K_{leaf}.

To better understand the implications of SSWU to plant function, we need to understand how water moves across the leaf surface and whether this process is affected by leaf hydration. The hydration status of the leaf surface can affect its permeability to water (Fernandez *et al.*, 2017), and thus affect the conductance of

the leaf surface to SSWU (K_{surf}), which may occur in liquid or gaseous form. Although Guzman-Delgado *et al.* (2018) documented temporal changes in K_{surf} during leaf rehydration, whether K_{surf} depends on leaf hydration status, as does K_{leaf}, remains untested.

We tested two novel hypotheses in *Avicennia marina*, a mangrove species that exhibits SSWU (Nguyen *et al.*, 2017b; Schreel *et al.*, 2019): that (1) K_{surf} declines with decreasing leaf water potential and (2) K_{leaf} recovers overnight through SSWU.

Materials and Methods

Sampling and processing

During two field campaigns in May and August 2018, one sun-exposed branch per tree, *c.* 20 mm diameter, was collected from eight individuals of *Avicennia marina* ssp. *eucalyptifolia* (Zipp. ex Moldenke) J. Everett growing on the south arm of the Daintree River (16° 17′ 20″ S, 145° 24′ 59″ E) for measurements of K_{leaf}; five individuals from the same populations were used to build pressure–volume (PV) curves and to estimate K_{surf}. Branches were collected at *c.* 1 m above the maximum tide level from trees *c.* 6 m tall. Soil water (collected at a depth of 30 cm) and surface water salinity at the sampling site were determined in August using a refractometer (AST, Tokyo, Japan). Soil water salinity (at a depth of 30 cm) averaged 25 ppt ($n = 2$), and surface water salinity was 24.3 ± 0.2 ppt ($n = 5$, Table 1), equivalent to osmotic potentials of −1.71 MPa and -1.66 ± 0.1 MPa, respectively. The climate in the study site is classified as a tropical monsoon climate (Am) under the definition of Köppen (1936).

Sampling of branches took place between 16:00 and 18:00 h. Immediately after cutting, branches were placed in black plastic bags and brought to the laboratory within 30 min, where they were recut under a solution of 5% seawater and left to rehydrate overnight; the solution salinity was based on measured xylem sap concentrations in this species (Ball, 1988; Stuart *et al.*, 2007). Suspended matter was allowed to settle from fresh seawater before the desired amount was decanted into fresh water to prepare the 5% seawater solution. The day after collection, the branches were recut into twigs bearing *c.* 10–20 leaves and maintained with the cut ends in the solution under dark, nontranspiring conditions.

Table 1 Water salinity at the sampling site and physical properties of leaves of *Avicennia marina* ssp. *eucalyptifolia* used for constructing pressure–volume (PV) curves

Variable	Symbol	Units	Mean	SE
Surface water salinity	—	ppt	24.3	0.2
Soil water salinity	—	ppt	25	—
Leaf area	LA	cm^2	19.8	1.21
Saturated weight	SW	g	0.89	0.06
Dry weight	DW	g	0.28	0.02
Leaf dry mass per area	LMA	$g\,m^{-2}$	139	1.86
Saturated leaf water content per area	WCA_{sat}	$g\,m^{-2}$	312	7.44
Saturated leaf water content per dry mass	WCD_{sat}	$g\,g^{-1}$	2.25	0.05
Water potential at the turgor loss point	Ψ_{TLP}	MPa	−3.44	0.1
Osmotic potential at full turgor	Π_{ft}	MPa	−2.89	0.09

$n = 5$ for all measurements except soil water salinity ($n = 2$).

Pressure–volume (PV) curves

One leaf from each of five trees was used to construct a PV curve (Tyree & Richter, 1981). Measurements of leaf weight and leaf water potential (Ψ_{leaf}) were made at intervals corresponding to a decrease of 10 to 20 mg in fresh weight (FW) using a 1 mg resolution balance (ML303E; Mettler-Toledo GmbH, Greifensee, Switzerland) and a pressure chamber (1505D; PMS Instruments, Corvallis, OR, USA). All leaves were scanned with a CanoScan LiDe 110 (Canon Inc., Tokyo, Japan) for measurement of leaf area (Adobe PHOTOSHOP CC; Adobe Systems, San José, CA, USA). Leaf dry weight (DW) was determined after oven-drying at 70°C for 48 h using a 0.1 mg resolution balance (AX205, Mettler-Toledo GmbH). Relative water content (RWC) was calculated as

$$RWC = \frac{FW - DW}{SW - DW} \times 100 \qquad \text{Eqn 1}$$

where FW is the leaf fresh weight (in grams), DW is the leaf dry weight (in grams) and SW is the leaf saturated weight (in grams) (i.e. the maximum FW measured for each leaf after rehydrating). The water potential at the turgor loss point (Ψ_{TLP}) was determined as the highest Ψ_{leaf} value on the linear domain of the plot between the inverse of leaf water potential ($1/\Psi_{leaf}$) and relative water deficit (100 − RWC). For determination of the osmotic potential at full turgor (Π_{ft}), we excluded the apoplastic water fraction for the first domain of the PV curve, as in Nguyen *et al.* (2017b) (see Supporting Information Fig. S1).

Because *Avicennia marina* leaves exhibit a three-domain PV curve (Nguyen *et al.*, 2017a,b), leaf capacitance between full hydration and the Ψ_{TLP} was determined as the first derivative of a third-order polynomial function fitted to the values of RWC and Ψ_{leaf} from all curves ($RWC = 102.17 - 18.22 \times \Psi_{leaf} + 8.01 \times \Psi_{leaf}^2 - 1.3 \times \Psi_{leaf}^3$; $r^2 = 0.91$; $P < 0.0001$). As the solution used for plant tissue hydration was always 5% seawater (equivalent to a water potential of −0.12 MPa), the curve fitting was made with the constraint that it must pass through (0.12, 100). At values of $\Psi_{leaf} < \Psi_{TLP}$, capacitance was obtained from a straight line fitted to the values of RWC and Ψ_{leaf} ($RWC = 111.82 - 8.88 \times \Psi_{leaf}$; $r^2 = 0.5$; $P < 0.0001$) with the constraint that it must intersect the value of the polynomial fit at the Ψ_{TLP}.

Shoot surface water uptake (SSWU) kinetics

The rates of SSWU were determined by placing excised branches in a plastic chamber kept at saturating humidity (see Rehydration kinetics section for details) and by tracking changes in Ψ_{leaf}, using the same principle as the rehydration kinetics method (RKM) method (Brodribb & Holbrook, 2003), i.e. estimating changes in mass through PV-curve derived capacitance values and relaxation of Ψ_{leaf}. Working with attached leaves enabled us to study the rates of

SSWU in branches which were treated in the same way as for the RKM measurements (see Rehydration kinetics section). However, our experimental design does not distinguish the organ taking up the water, and thus SSWU may also involve water absorbed by bark (Mason Earles *et al.*, 2016). Five branches (one per tree) were cut into three branchlets and randomly assigned to each of three different dehydration levels corresponding to water potentials of -3.2 ± 0.1, -3.9 ± 0.1 and -4.9 ± 0.1 MPa (mean ± SE), after which they were sprayed with rainwater until dripping and placed in the chambers. Thus, Ψ_{leaf} measurements were made on two leaves per branch after 30 min and then every hour for the next 4 h. Most branches were equilibrated before the start of the experiment, as the difference in Ψ_{leaf} within branches was < 0.1 MPa in all but two branches (in which $\Delta\Psi_{leaf}$ was 0.24 and 0.26 MPa). After each measurement, branches were sprayed until dripping and placed back into the chambers. The last measurement was made 12 h from the start. All measurements were started at night (*c.* 20:00 h).

In one of the treatments (−3.2 MPa starting Ψ_{leaf}), the salinity of the water on the leaf surface was determined for each of the five replicate branches at each time point by gently rubbing 3–5 leaves on a refractometer (AST), until a continuous film of water was collected. The measured salinity values were then converted to osmotic potentials and used for calculating the gradient driving water movement into the leaf. Time-dependent variation in Ψ_{leaf} and in osmotic potential of leaf surface water were fitted with an exponential decay function of the form

$$\Psi = \Psi_f + A \times e^{-\frac{t}{\tau}} \quad \text{Eqn 2}$$

where Ψ_f is the final Ψ_{leaf}, A is the function amplitude constant, τ is the function time constant and t is the time since the start of the experiment (in hours).

The cumulative amount of water taken up per unit leaf area (SSWU, mol H_2O m^{-2}) in response to SSWU was estimated using the functions fitted to the PV curves, and corrected for the water content per unit area as:

$$SSWU = \left(RWC(\Psi_{leaf})_t - RWC(\Psi_{leaf})_0\right) \times \frac{1}{100} \times WCA_{sat} \times \frac{1}{M} \quad \text{Eqn 3}$$

where $RWC(\Psi_{leaf})_t$ is the value of the function fitted to the data from PV curves evaluated at the Ψ_{leaf} measured at times $t = 0.5$, 1.5, 2.5, 3.5, 4.5 and 12 h and WCA_{sat} is the saturated leaf water content per unit area (in g m^{-2}). The change in moles of water was thus calculated between each measurement of Ψ_{leaf}. Conductance to SSWU (K_{surf}, μmol H_2O m^{-2} s^{-1} MPa^{-1}) was calculated between each time point as:

$$K_{surf} = \frac{SSWU_t - SSWU_{t-1}}{S_t - \Psi_{leaf\,t}} \times \frac{1}{\Delta t} \quad \text{Eqn 4}$$

where S_t (in MPa) was the estimated value for the osmotic potential of the leaf surface water obtained from the exponential decay function fitted to the data of one of the SSWU treatments (−3.2 MPa; $S_t = 1.02 \times e^{(-t/1.82)} + 0.37$; $r^2 = 0.88$; $P = 0.003$) evaluated at each time point, and Δt is the time between each pair of measurements (in seconds).

Rehydration kinetics

The K_{leaf} value was determined with a modified version of the RKM (Brodribb & Holbrook, 2003), which estimates water fluxes based on Ψ_{leaf} relaxation kinetics in response to rehydration and leaf capacitance values derived from the PV curve.

To construct leaf vulnerability curves, branches were bench dried to different levels of Ψ_{leaf} and left to equilibrate in black plastic bags for 30 min, after which the initial Ψ_{leaf} was measured. Subsequently, six leaves from the same branch were cut with the petiole submerged under a 5% seawater solution and left to rehydrate for periods of 30, 60, 120, 240, 300 and 480 s. Following these time periods, leaves were equilibrated in bags in the dark for *c.* 10 min, after which Ψ_{leaf} was measured and K_{leaf} calculated as

$$K_{leaf} = \frac{C_{leaf}\, log_e\left(\frac{\Psi_0}{\Psi_t - \Psi_s}\right)}{t} \quad \text{Eqn 5}$$

where C_{leaf} is leaf area normalized capacitance calculated from the PV curve function evaluated at Ψ_t (in mol H_2O m^{-2} $MPa^{-}1$, see Eqn 6), t is the duration of rehydration (in seconds), Ψ_0 is the leaf water potential before rehydration (in MPa), Ψ_t is the leaf water potential at time t (in MPa) and Ψ_s is the osmotic potential of the water source (−0.12 MPa). The last term corrects for the fact that $\Psi_t < \Psi_s$ (Supporting Information Notes S1). The C_{leaf} value was calculated for each value of Ψ_t as

$$C_{leaf} = \frac{dRWC}{d\Psi_{leaf}} \times \frac{1}{100} \times WCA_{sat} \times \frac{1}{M} \quad \text{Eqn 6}$$

where $dRWC/d\Psi_{leaf}$ is the derivative of the PV function evaluated at Ψ_t and M is the molar mass of water (in g mol^{-1}). As K_{leaf} is a function of C_{leaf}, the relaxation time constant of Ψ_{leaf} (k) was calculated as

$$k = \frac{\log_e\left(\frac{\Psi_0}{\Psi_t - \Psi_s}\right)}{t} \quad \text{Eqn 7}$$

to test if leaf hydraulic recovery was dependent on the different values of C_{leaf}.

The same method described for constructing vulnerability curves was used for measuring changes in K_{leaf} in response to SSWU. After reaching a value of Ψ_{leaf} at which considerable K_{leaf} was lost (-3.8 ± 0.1 MPa), each of eight equilibrated branches was cut in two using pruning clippers. Half of these branches were used for measuring K_{leaf} in this partially dehydrated state, and the other half were placed in a 50 L polypropylene container at saturating humidity, sprayed once with water and left to rehydrate through SSWU overnight. The container was kept humid by a *c.* 5 cm film of water in the bottom with semi-submerged wads of sponge to increase evaporative surface area. Branches were kept suspended inside the box so that the cut ends were not

in contact with free water. Leaves were visibly wet the next morning. The K_{leaf} value was then measured for these half-branches as described earlier. The procedure was repeated for eight branches at a more severely dehydrated state (-4.9 ± 0.1 MPa), with the addition of an unsprayed control treatment. To account for the possibility of leaves taking up water from stem tissues in the -3.8 MPa treatment, an unsprayed control treatment was added (April 2019) for a set of eight branches at a similar starting water potential (-3.9 ± 0.1 MPa) ($F_{1,14} = 1.62$, $P = 0.23$, one-way analysis of variance (ANOVA)). Unsprayed controls were kept in plastic bags with no addition of water.

The vulnerability curve obtained from the RKM measurements during dehydration was fitted with a sigmoidal function (Pammenter & Van der Willigen, 1998) of the form

$$K_{leaf} = \frac{K_{max}}{1 + e^{a(\Psi_{leaf} - \Psi_{50})}} \quad \text{Eqn 8}$$

where K_{max} is the estimated maximum value of K_{leaf}, a is the function rate constant and Ψ_{50} is the water potential at which 50% K_{leaf} has been lost.

Data analyses

The differences in k, K_{leaf} and Ψ_{leaf} between before and after SSWU were analysed using paired t-tests using GENSTAT 18.2 (VSN International, Hemel Hempstead, UK) under the null hypothesis that there were no differences before and after SSWU. All plots and nonlinear models were generated using ORIGINPRO 2017 (OriginLab, Northampton, MA, USA) and stylized in Adobe ILLUSTRATOR CC (Adobe Systems). Models were fitted using the Levenberg–Marquardt algorithm and validated via normal distribution of the residuals. The effects of time and starting Ψ_{leaf} on SSWU and K_{surf} were analysed using linear mixed-effects models in R (v.3.5.1, the R Foundation for Statistical Computing, Vienna, Austria) using the LME4 and LMERTEST packages. The standard error of WCA_{sat} and the 95% confidence interval of the function fitted to PV curve data (PV.CI) were propagated throughout the calculations of SSWU and K_{surf}. To test if the sources of error had any effects on the results, the models were also run using the higher and lower bounds of the estimates of SSWU and K_{surf} based on the error terms derived from PV.CI and WCA_{sat}. The model used for SSWU and K_{surf} was initial Ψ_{leaf} × rehydration time; plant individual was considered as a random effect. Models for SSWU and K_{surf} were run using all time points (0–12 h) or the time points from 0 to 4.5 h, as SSWU ceased after 4.5 h in all treatments. Results of K_{surf} are discussed excluding the last time point, but the results of both analyses are presented later. Results of these models are included in Supporting Information Tables S1 and S2.

Results

Continuous variation in leaf capacitance

Leaf capacitance varied 10-fold from 3.15 mol H_2O m^{-2} MPa^{-1} at full hydration to 0.31 mol H_2O m^{-2} MPa^{-1} at the capacitance function inflection point (−2.05 MPa; Fig. 1a). Fitting a polynomial function for points in domains 1 and 2 resulted in a lower goodness-of-fit than those obtained by fitting linear functions for

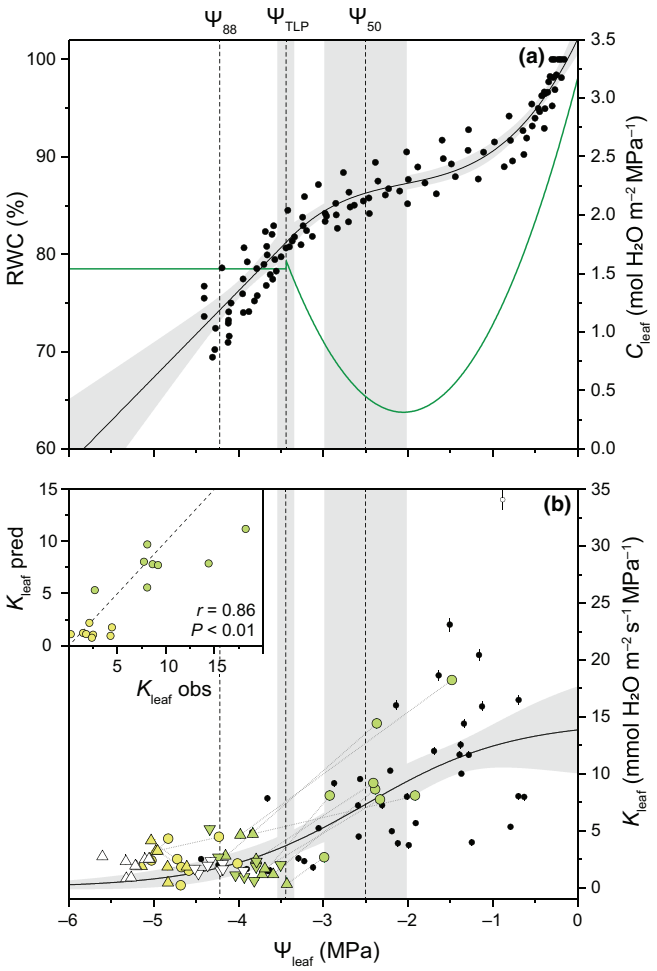

Fig. 1 (a) Pressure–volume (PV) curves from *Avicennia marina* ssp. *eucalyptifolia* and capacitance (C_{leaf}) values used for calculation of leaf hydraulic conductance (K_{leaf}) and conductance to shoot surface water uptake. Black dots correspond to values from five plants. The black curve corresponds to the polynomial and linear models fitted to the PV curve data at leaf water potential (Ψ_{leaf}) higher than the leaf water potential at the turgor-loss point (Ψ_{TLP}) and $\Psi_{leaf} < \Psi_{TLP}$, respectively. The green curve corresponds to the leaf area standardized capacitance values derived from the PV curve fit (i.e. the slope of the estimated leaf relative water content vs Ψ_{leaf}). (b) Loss and recovery of K_{leaf} in response to dehydration and shoot surface water uptake (SSWU). Black dots and triangles correspond to data points measured during dehydration; circles correspond to measurements performed after SSWU. Filling colour indicates starting Ψ_{leaf} at −3.8 MPa or −3.9 MPa (light green) and −4.9 MPa (yellow). Open triangles correspond to controls (i.e. no spraying) treatments. Error bars correspond to the uncertainty term propagated from the saturated leaf water content per unit area measurements. Dotted lines indicate the change in Ψ_{leaf} and K_{leaf} for each individual. Dashed lines indicate the water potential at 50% loss of K_{leaf} (Ψ_{50}), Ψ_{TLP} and the water potential at 88% loss of K_{leaf} (Ψ_{88}). Grey areas indicate the 95% confidence interval for the model and the SE of the Ψ_{50} and Ψ_{TLP}. The open circle corresponds to an outlier measured during dehydration (Grubb's test, $P < 0.05$) and was not included in the model. Inset: correlation between observed and predicted K_{leaf} values measured after the SSWU treatment; the dashed line depicts the 1 : 1 relation between observed and predicted values.

each domain (root mean square error (RMSE) = 1.59 from linear functions, Fig. S2; RMSE = 1.67 from polynomial function, Fig. 1a). However, because C_{leaf} was derived from the PV curve function, variation in C_{leaf} was continuous with no disjunction in C_{leaf} at the Ψ_{TLP} or at the transition between domain 1 and 2 (Figs 1a, S2).

Kinetics of SSWU

As expected from SSWU, Ψ_{leaf} increased through time in all treatments (Fig. 2a; Table S3). Leaf surface salinity decreased with time, presumably due to salts being washed off with spraying. However, none of the leaves achieved full hydration via SSWU, and Ψ_{leaf} values were always more negative than the osmotic potential in the leaf surface (i.e. the maximum achievable Ψ_{leaf}).

The recovery of Ψ_{leaf} corresponded to increases in leaf mass through time in all treatments ($F_{81.98} = 6.13$, $P = 0.02$) (Fig. 2b). Leaves absorbed 0.5–1.2 mol H_2O m^{-2} over a period of 12 h; in all cases, > 98% of the total water uptake occurred within the first 4.5 h. The effect of Ψ_{leaf} on SSWU was not significant between 0 and 4.5 h ($F_{82.37} = 3.07$, $P = 0.08$); however, when considering all time points (0–12 h), Ψ_{leaf} had a significant effect on SSWU ($F_{96.66} = 7.42$, $P = 0.01$) (Fig. 2b; Table S1). The significant effect of Ψ_{leaf} on SSWU was consistent across all analyses, independent of the bounds of the sources of error used in calculations (Table S2).

The values of K_{surf} declined with time ($F_{71} = 4.66$, $P = 0.03$), reaching negligible values after 3 h (Fig. 2c). The initial Ψ_{leaf} had no significant effect on K_{surf} over the first 4.5 h ($F_{71} = 2.96$, $P = 0.09$) (Fig. 2c, inset), and the effect was also nonsignificant at 0.5 h (i.e. initial K_{surf}) ($F_{9.33} = 2.56$; $P = 0.14$). However, the significance of the effect of Ψ_{leaf} on K_{surf} was dependent on the bounds of the sources of error used in calculations (Table S2). On average, K_{surf} in the −4.9 MPa treatment was < 50% of that in the −3.2 and −3.9 MPa treatments during the first 2 h (Fig. 2c). There was no significant interaction between initial Ψ_{leaf} and rehydration time over the first 4.5 h ($F_{71} = 1.72$, $P = 0.19$; Fig. 2c).

Effects of dehydration and SSWU on K_{leaf}

The K_{leaf} value of *Avicennia marina* declined with decreasing Ψ_{leaf} during branch dehydration (Fig. 1b). When dehydrated branches were sprayed with water, SSWU led to a significant increase in Ψ_{leaf} overnight (Table 2); when unsprayed, all branches dehydrated overnight, as evidenced by a significant decrease in Ψ_{leaf} (Table 2). For branches dehydrated to an initial state of −3.8 MPa, SSWU led to an increase in K_{leaf} from 2.36 to 9.63 mmol H_2O m^{-2} s^{-1} MPa^{-1} (i.e. from 16% to 66% of the estimated K_{max}; Table 2; Table S3). However, in branches dehydrated to −4.9 MPa, K_{leaf} did not increase significantly whether sprayed or unsprayed (Table 2). These results were not due to differences in C_{leaf} (Fig. 1a); when calculated independent of C_{leaf}, the changes in the rehydration time constant exhibited a similar pattern to those of K_{leaf} (Fig. S3).

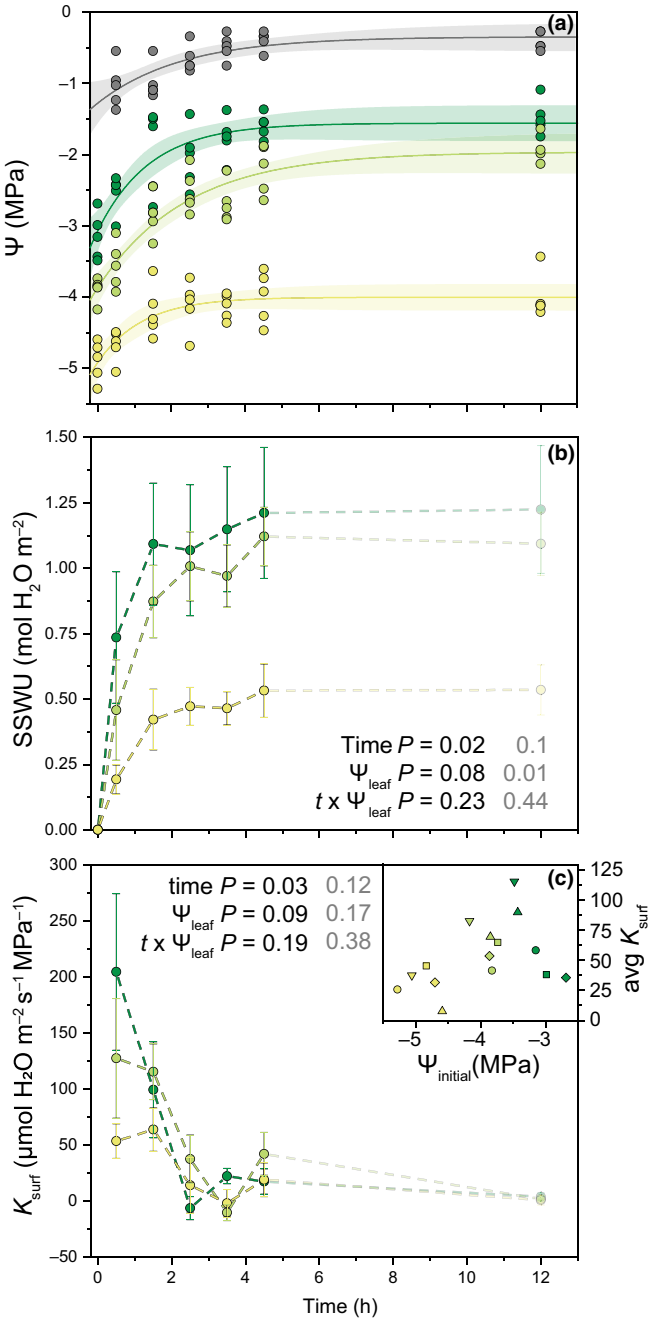

Fig. 2 Measured changes in leaf water potential (Ψ_{leaf}, coloured symbols) and leaf surface osmotic potential (grey symbols) (a), and estimated changes in fresh mass (b) and conductance to shoot surface water uptake (K_{surf}; c) during a 12-h period of intermittent spraying. All models in (a) correspond to exponential decay functions (Eqn 2) and the parameters fitted by each model are presented in Supporting Information Table S4. For (b), shoot surface water uptake (SSWU) was calculated according to Eqn 3, and for (c) K_{surf} was calculated according to Eqn 4. The inset in (c) corresponds to the average K_{surf} values between 0 and 4.5 h for each individual (represented by different symbols). Colour depicts the starting leaf water potential of each treatment at −3.2 MPa (dark green), −3.9 MPa (light green) and −4.9 MPa (yellow). Error bars correspond to ± SE. The *P* values shown are from linear mixed models considering all time points (grey) or excluding the data at *t* = 12 h (black). *n* = 5.

While we observed more recovery of Ψ_{leaf} than K_{leaf} in response to SSWU, the values of K_{leaf} observed before and after spraying treatments accorded with those predicted by the model based on Ψ_{leaf} ($r = 0.86$, $P < 0.01$; Fig. 1b, inset). Thus, the non-significant changes in K_{leaf} in the −4.9 MPa dehydration treatment were consistent with insufficient rehydration through SSWU.

Discussion

A functional significance of SSWU was demonstrated by recovery of K_{leaf} in *Avicennia marina*. Notably, SSWU was dependent on leaf hydration, although the response of K_{surf} to Ψ_{leaf} was not significant. These results provide evidence to guide future research into the role of SSWU in diel K_{leaf} recovery in plants subject to regular leaf wetting events.

Kinetics of SSWU

Our results revealed that K_{surf} varied with time, consistent with Guzman-Delgado *et al.* (2018), and there was no effect of the initial Ψ_{leaf} on K_{surf}, despite significant effects of initial Ψ_{leaf} on SSWU. For the purposes of discussion, we assume that most surface water is absorbed through leaves. Because the maximum K_{leaf} was *c.* 72 times higher than the maximum K_{surf} (Figs 2c, 1b), SSWU is likely dominated by the permeability of the leaf surface, and not by the hydraulic conductance within the mesophyll. Assuming that the resistances to water movement through the mesophyll during SSWU correspond to those outside the xylem pathway, and that they correspond to *c.* $0.5/K_{leaf}$ (Scoffoni *et al.*, 2017b), we calculate that the resistance of water movement across the leaf surface would be *c.* 26–40 times greater than that through the mesophyll; if the resistances within the xylem were incorporated, then leaf surface resistance would be *c.* 13–19 times greater than that of the mesophyll, depending on leaf hydration status (Notes S2). These values agree with those found by Guzman-Delgado *et al.* (2018) in detached leaves of *Prunus dulcis* and *Quercus lobata*, in which the leaf surface resistance was 21–30 times greater than that of the petiole. Thus, SSWU is mainly determined by leaf surface permeability.

Although the permeability of the cuticle may be affected by its hydration status (Fernandez *et al.*, 2017), we observed no effect of Ψ_{leaf} on K_{surf}. Dehydration-dependent changes in the hydraulic conductance within the mesophyll (Fig. 1b) may not be reflected in changes in K_{surf}, as the latter largely depends on leaf surface permeability. While the effects of Ψ_{leaf} on K_{surf} were dependent on the sources of error used in calculations, the decline of K_{surf} with time is also inconsistent with hydration status determining cuticle permeability because all plants rehydrated during leaf wetting. It is possible that K_{surf} in *Avicennia* is not governed by cuticle permeability, but regulated by epidermal features such as stomata (Eichert *et al.*, 2008), trichomes (Nguyen *et al.*, 2017b) or salt glands (Tan *et al.*, 2013), whose contribution to K_{surf} may vary with time. The decline in K_{surf} with rehydration time was consistent with Guzman-Delgado *et al.* (2018), who reported a decreasing K_{surf} with time due to incomplete relaxation of Ψ_{leaf} in *Prunus dulcis* and *Quercus lobata*. While salt glands have been shown to take up water in *Avicenna officinalis* (Tan *et al.*, 2013), the lack of salt glands in *Prunus dulcis* and *Quercus lobata* suggests the temporal decline in K_{surf} is regulated via a common mechanism. Further work needs to determine the pathways of SSWU, with particular attention to stomata, and quantify how these are related to the temporal changes in K_{surf} during rehydration.

Our data were comparable to those reported for detached leaves of *Prunus dulcis*, for which the estimated maximum K_{surf} was *c.* 90 μmol m^{-2} s^{-1} MPa^{-1} (Guzman-Delgado *et al.*, 2018), while our values for *Avicennia marina* ranged from *c.* 60 to 200 μmol m^{-2} s^{-1} MPa^{-1} depending on the initial Ψ_{leaf} (Fig. 2c); the time required until SSWU ceased and the amount of water taken up by the leaves were also similar. In contrast to Guzman-Delgado *et al.* (2018), *Avicennia marina* leaves were rehydrated while attached to stems and K_{surf} estimated based on changes in Ψ_{leaf}. Consequently, because estimates of C_{leaf} come from detached leaves, K_{surf} values were potentially underestimated because the relaxation kinetics of Ψ_{leaf} may have been quenched by water moving from leaves into stems.

Effects of dehydration and SSWU on K_{leaf}

Our results showed that K_{leaf} can recover through SSWU. After spraying with water, K_{leaf} increased with Ψ_{leaf} along the same plotted path as observed during dehydration (Fig. 1b, inset). These results contrast with data available from other studies in which rehydration occurred via the roots. Several studies reported that recovery of K_{leaf} depends on the extent of leaf dehydration (Bucci *et al.*, 2003; Lo Gullo *et al.*, 2003; Brodribb & Holbrook, 2004; Hao *et al.*, 2008; Johnson *et al.*, 2009; Yang *et al.*, 2012). Some studies found that loss of K_{leaf} occurs mainly through reversible loss of conductance outside the xylem, and that

Table 2 Changes in leaf water potential (Ψ_{leaf}) and leaf hydraulic conductance (K_{leaf}) measured overnight under conditions of spraying (+) and no spraying (−)

Ψ_{leaf} (MPa)	SSWU	$\Delta\Psi_{leaf}$ (MPa)	*P*-value	ΔK_{leaf} (mmol m^{-2} s^{-1} MPa^{-1})	*P*-value
−3.8	+	1.42 ± 0.1	< 0.001	7.23 ± 1.25	0.001
−3.9	−	−0.22 ± 0.08	0.021	−0.13 ± 0.54	0.826
−4.9	+	0.33 ± 0.06	0.001	0.03 ± 0.4	0.954
−4.9	−	−0.34 ± 0.03	< 0.001	−0.63 ± 0.45	0.231

Values correspond to the mean ± SE difference between the initial and final measurements. *P*-values correspond to contrasts obtained from paired *t*-tests. $n = 8$.

embolism in leaves is rare until extreme dehydration (Scoffoni *et al.*, 2017a) and studies with more severe water stress found evidence of irreparable xylem embolism associated with the loss of K_{leaf} (Brodribb *et al.*, 2016; Johnson *et al.*, 2018). Loss of conductance in other organs such as roots and stems might also affect the recovery of K_{leaf}. Creek *et al.* (2018) found lower K_{leaf} recovery than that expected from Ψ_{leaf} recovery (i.e. irreversible loss) in plants in which losses of hydraulic conductance also took place in roots and stems. It is possible that rehydration through the leaf surface may enable plants to bypass the limitations imposed by embolized conduits in root and stem xylem, thereby enabling K_{leaf} recovery. Thus, SSWU may play an important role in K_{leaf} recovery when rehydration from the soil is limited by the availability of soil water or the capacity for water transport. Further research is needed to extend the role of SSWU in leaf hydraulic recovery to the wide range of conditions in which SSWU has been documented (reviewed in Berry *et al.*, 2018). Our findings suggest that the dependence of SSWU on leaf hydration status would limit the range of conditions under which SSWU is functionally significant for hydraulic recovery. Future studies should determine the mechanisms by which hydraulic conductance can recover via SSWU in leaves and whether leaf xylem refilling is involved.

Conclusion

We found two results in the mangrove species *Avicennia marina* that advance understanding of SSWU and its physiological effects. First, SSWU depended on leaf hydration status, although there was no significant effect of Ψ_{leaf} on K_{surf}. Second, leaf hydraulic conductance (K_{leaf}) lost through dehydration was recovered by shoot absorption of liquid water. The recovery of K_{leaf} via SSWU depended on leaf water potential and retraced the same path as K_{leaf} loss in response to dehydration. Given the prevalence of SSWU across diverse plant species and ecosystems (Dawson & Goldsmith, 2018), our results support recent assertions (Schreel & Steppe, 2019) on the importance of leaf wetting events in the maintenance of leaf gas exchange and plant productivity, which may affect plant fitness under changing climatic scenarios.

Acknowledgements

The authors thank the Australian Research Council for financial support, granted to MCB, LS and RSO (DP180102969). TIF was supported by the Becas Chile PhD scholarship programme granted by CONICYT. The authors thank Catherine Bone and Nigel Brothers for exceptional field support and accommodation at the Daintree River, and John R. Evans for thoughtful comments on the manuscript.

Author contributions

TIF and MCB conceived the study and designed the experiments; TIF, LIO and CJB collected the data; TIF analysed the data with suggestions from H-JY, LS and MCB, TIF wrote the manuscript with input from MCB, LS, CJB, RSO, LIO and H-JY.

ORCID

Marilyn C. Ball https://orcid.org/0000-0001-9170-940X
Tomás I. Fuenzalida https://orcid.org/0000-0002-8353-5080
Rafael S. Oliveira https://orcid.org/0000-0002-6392-2526
Lawren Sack https://orcid.org/0000-0002-7009-7202
Hwan-Jin Yoon https://orcid.org/0000-0003-1772-7911

References

Ball MC. 1988. Salinity tolerance in the mangroves *Aegiceras corniculatum* and *Avicennia marina*. I. Water use in relation to growth, carbon partitioning, and salt balance. *Functional Plant Biology* **15**: 447–464.

Berry ZC, Emery NC, Gotsch SG, Goldsmith GR. 2018. Foliar water uptake: processes, pathways, and integration into plant water budgets. *Plant, Cell & Environment* **42**: 410–423.

Blackman CJ, Brodribb TJ, Jordan GJ. 2009. Leaf hydraulics and drought stress: response, recovery and survivorship in four woody temperate plant species. *Plant, Cell & Environment* **32**: 1584–1595.

Brodribb TJ, Cochard H. 2009. Hydraulic failure defines the recovery and point of death in water-stressed conifers. *Plant Physiology* **149**: 575–584.

Brodribb TJ, Holbrook NM. 2003. Stomatal closure during leaf dehydration, correlation with other leaf physiological traits. *Plant Physiology* **132**: 2166–2173.

Brodribb T, Holbrook NM. 2004. Diurnal depression of leaf hydraulic conductance in a tropical tree species. *Plant, Cell & Environment* **27**: 820–827.

Brodribb TJ, Skelton RP, McAdam SA, Bienaime D, Lucani CJ, Marmottant P. 2016. Visual quantification of embolism reveals leaf vulnerability to hydraulic failure. *New Phytologist* **209**: 1403–1409.

Bucci S, Scholz F, Goldstein G, Meinzer F, Sternberg LdS. 2003. Dynamic changes in hydraulic conductivity in petioles of two savanna tree species: factors and mechanisms contributing to the refilling of embolized vessels. *Plant, Cell & Environment* **26**: 1633–1645.

Creek D, Blackman CJ, Brodribb TJ, Choat B, Tissue DT. 2018. Coordination between leaf, stem, and root hydraulics and gas exchange in three arid-zone angiosperms during severe drought and recovery. *Plant, Cell & Environment* **41**: 2869–2881.

Dawson TE, Goldsmith GR. 2018. The value of wet leaves. *New Phytologist* **219**: 1156–1169.

Eichert T, Kurtz A, Steiner U, Goldbach HE. 2008. Size exclusion limits and lateral heterogeneity of the stomatal foliar uptake pathway for aqueous solutes and water-suspended nanoparticles. *Physiologia Plantarum* **134**: 151–160.

Eller CB, Lima AL, Oliveira RS. 2016. Cloud forest trees with higher foliar water uptake capacity and anisohydric behavior are more vulnerable to drought and climate change. *New Phytologist* **211**: 489–501.

Fernandez V, Bahamonde HA, Javier Peguero-Pina J, Gil-Pelegrin E, Sancho-Knapik D, Gil L, Goldbach HE, Eichert T. 2017. Physico-chemical properties of plant cuticles and their functional and ecological significance. *Journal of Experimental Botany* **68**: 5293–5306.

Flexas J, Carriqui M, Nadal M. 2018. Gas exchange and hydraulics during drought in crops: who drives whom? *Journal of Experimental Botany* **69**: 3791–3795.

Guzman-Delgado P, Mason Earles J, Zwieniecki MA. 2018. Insight into the physiological role of water absorption via the leaf surface from a rehydration kinetics perspective. *Plant, Cell & Environment* **41**: 1886–1894.

Hao GY, Hoffmann WA, Scholz FG, Bucci SJ, Meinzer FC, Franco AC, Cao KF, Goldstein G. 2008. Stem and leaf hydraulics of congeneric tree species from adjacent tropical savanna and forest ecosystems. *Oecologia* **155**: 405–415.

Johnson DM, Woodruff DR, McCulloh KA, Meinzer FC. 2009. Leaf hydraulic conductance, measured *in situ*, declines and recovers daily: leaf hydraulics, water potential and stomatal conductance in four temperate and three tropical tree species. *Tree Physiology* **29**: 879–887.

Johnson KM, Jordan GJ, Brodribb TJ. 2018. Wheat leaves embolized by water stress do not recover function upon rewatering. *Plant, Cell & Environment* **41**: 2704–2714.

Köppen W. 1936. Das Geographisches System der Klimate. In: Köppen W, Geiger R, eds. *Handbuch der Klimatologie v. 1, pt C*. Berlin, Germany: Gebruder, 1–46.

Lo Gullo MA, Nardini A, Trifilò P, Salleo S. 2003. Changes in leaf hydraulics and stomatal conductance following drought stress and irrigation in *Ceratonia siliqua* (Carob tree). *Physiologia Plantarum* **117**: 186–194.

Mason Earles J, Sperling O, Silva LC, McElrone AJ, Brodersen CR, North MP, Zwieniecki MA. 2016. Bark water uptake promotes localized hydraulic recovery in coastal redwood crown. *Plant, Cell & Environment* **39**: 320–328.

Mayr S, Schmid P, Laur J, Rosner S, Charra-Vaskou K, Damon B, Hacke UG. 2014. Uptake of water via branches helps timberline conifers refill embolized xylem in late winter. *Plant Physiology* **164**: 1731–1740.

Nguyen HT, Meir P, Sack L, Evans JR, Oliveira RS, Ball MC. 2017a. Leaf water storage increases with salinity and aridity in the mangrove *Avicennia marina*: integration of leaf structure, osmotic adjustment and access to multiple water sources. *Plant, Cell & Environment* **40**: 1576–1591.

Nguyen HT, Meir P, Wolfe J, Mencuccini M, Ball MC. 2017b. Plumbing the depths: extracellular water storage in specialized leaf structures and its functional expression in a three-domain pressure -volume relationship. *Plant, Cell & Environment* **40**: 1021–1038.

Pammenter Nv, Van der Willigen C. 1998. A mathematical and statistical analysis of the curves illustrating vulnerability of xylem to cavitation. *Tree Physiology* **18**: 589–593.

Sack L, Holbrook NM. 2006. Leaf hydraulics. *Annual Review of Plant Biology* **57**: 361–381.

Schreel JDM, Steppe K. 2019. Foliar water uptake changes the world of tree hydraulics. *npj Climate and Atmospheric. Science* **2**: 1.

Schreel JDM, Van de Wal BAE, Hervé-Fernandez P, Boeckx P, Steppe K. 2019. Hydraulic redistribution of foliar absorbed water causes turgor-driven growth in mangrove seedlings. *Plant, Cell & Environment* **42**: 2437–2447.

Scoffoni C, Albuquerque C, Brodersen C, Townes SV, John GP, Bartlett MK, Buckley TN, McElrone AJ, Sack L. 2017a. Outside-xylem vulnerability, not xylem embolism, controls leaf hydraulic decline during dehydration. *Plant Physiology* **173**: 1197–1210.

Scoffoni C, Chatelet DS, Pasquet-Kok J, Rawls M, Donoghue MJ, Edwards EJ, Sack L. 2016. Hydraulic basis for the evolution of photosynthetic productivity. *Nature Plants* **2**: 16072.

Scoffoni C, Sack L, Ort D. 2017b. The causes and consequences of leaf hydraulic decline with dehydration. *Journal of Experimental Botany* **68**: 4479–4496.

Stuart SA, Choat B, Martin KC, Holbrook NM, Ball MC. 2007. The role of freezing in setting the latitudinal limits of mangrove forests. *New Phytologist* **173**: 576–583.

Tan WK, Lin Q, Lim TM, Kumar P, Loh CS. 2013. Dynamic secretion changes in the salt glands of the mangrove tree species Avicennia officinalis in response to a changing saline environment. *Plant, Cell & Environment* **36**: 1410–1422.

Tyree MT, Richter H. 1981. Alternative methods of analysing water potential isotherms: some cautions and clarifications: I. The impact of non-ideality and of some experimental errors. *Journal of Experimental Botany* **32**: 643–653.

Wang X, Du T, Huang J, Peng S, Xiong D. 2018. Leaf hydraulic vulnerability triggers the decline in stomatal and mesophyll conductance during drought in rice. *Journal of Experimental Botany* **69**: 4033–4045.

Xiong D, Flexas J, Yu T, Peng S, Huang J. 2017. Leaf anatomy mediates coordination of leaf hydraulic conductance and mesophyll conductance to CO_2 in *Oryza*. *New Phytologist* **213**: 572–583.

Yang SJ, Zhang YJ, Sun M, Goldstein G, Cao KF. 2012. Recovery of diurnal depression of leaf hydraulic conductance in a subtropical woody bamboo species: embolism refilling by nocturnal root pressure. *Tree Physiology* **32**: 414–422.

Supporting Information

Additional Supporting Information may be found online in the Supporting Information section at the end of the article.

Fig. S1 Individual pressure–volume curves from *Avicennia marina* subsp. *eucaulyptifolia*.

Fig. S2 Pressure–volume curve as fitted with linear models for each domain and capacitance values derived from the linear fit.

Fig. S3 Time constants calculated from the exponential decay functions describing the relaxation of Ψ_{leaf} with rehydration time for each of the SSWU treatments.

Notes S1 Derivation of the equation used for calculating leaf hydraulic conductance.

Notes S2 Calculation of the relative contribution of leaf hydraulic resistance of the leaf surface to K_{surf}.

Table S1 ANOVA table for SSWU and K_{surf} considering the whole experimental period (0–12 h) or only the period in which SSWU took place (0–4.5 h).

Table S2 ANOVA table for SSWU and K_{surf} using the lower and higher bounds of WCA_{sat} and PV.CI for calculations.

Table S3 Fitting results for the three-parameter logistic models fitted to K_{leaf} data.

Table S4 Fitting results for the exponential decay models fitted to Ψ_{leaf} and leaf surface osmotic potential data used for calculating K_{surf}.

Please note: Wiley Blackwell are not responsible for the content or functionality of any Supporting Information supplied by the authors. Any queries (other than missing material) should be directed to the *New Phytologist* Central Office.